

Estimation of Nonlinear Aerodynamic Roll Models for Identification of Uncommanded Rolling Motions

C. Edward Lan* and Silvia Bianchi†
University of Kansas, Lawrence, Kansas 66045

and
Jay M. Brandon‡

NASA Langley Research Center, Hampton, Virginia 23681

DOI: 10.2514/1.30388

Detailed analysis of wind-tunnel data in free-to-roll testing of one aircraft model, the preproduction F/A-18E, in a transonic tunnel is presented. The main purpose is to identify possible uncommanded rolling motions of the full-scale aircraft by examining the roll dynamic characteristics of the model in the tunnel. To improve the tunnel balance data, the bearing-friction effect on the balance rolling-moment coefficient was removed. The corrected rolling-moment coefficients are then modeled through a fuzzy-logic algorithm. The resulting aerodynamic models are employed in calculating all roll derivatives by a central-difference scheme. The proposed wing-drop theory relies on the values of the relative aerodynamic stiffness in the rolling equation of motion, which is assumed to be composed of two terms: derivatives with respect to the roll angle alone and second-order derivatives of the rolling-moment coefficient with respect to the roll angle and angle of attack. Wing drop is predicted if the relative aerodynamic stiffness changes sign from that of the overall motion and if the contributions to the rolling-moment coefficient from both the first-order and second-order derivatives are of the same sign and are small in value. This is equivalent to the vanishing of a frequency with damping in the vibration theory. It is found that at a low angle of attack and a transonic Mach number, the dynamic motion is wing rock. As the angle of attack is increased, the wing-drop condition is initially exhibited with a single event, then with multiple occurrences of wing drop at a higher angle of attack, with the magnitude of roll-off angles changing with time. It is also found that wing-rock motion in the tunnel on a free-to-roll test rig is mostly caused by the unstable effect of time rate of sideslip angle, not by the traditional roll damping due to roll rate.

Nomenclature

b	= wing span
C_l	= rolling-moment coefficient (rolling moment divided by $\bar{q}Sb$)
C_{lp}	= $\delta C_l / \delta (pb/2V)$
$(C_{lp})_{osc}$	= $C_{lp} + C_{l\beta} \sin \alpha$
$C_{l\alpha\phi}$	= $\partial^2 C_l / \partial \alpha \partial \phi$
$C_{l\beta}$	= $\partial C_l / \partial \beta$
$C_{l\dot{\beta}}$	= $\partial C_l / \partial (\dot{\beta}b/2V)$
$C_{l\phi}$	= $\partial C_l / \partial \phi$
M	= Mach number
\bar{q}	= dynamic pressure
R^2	= square of multiple correlation coefficient
S	= wing area
t	= time
α_i	= initial angle of attack, deg
β	= sideslip angle
$\Delta(C_l)$	= contributions to the total rolling-moment coefficient from roll derivatives
δ_a	= aileron deflection angle
δ_{le}	= leading-edge flap deflection angle
δ_{te}	= trailing-edge flap deflection angle
θ	= pitch attitude angle

μ	= friction coefficient of bearing
ϕ	= roll angle
ψ	= phase angle

I. Introduction

DURING flight-testing of the preproduction F/A-18E aircraft in transonic conditions, unexpected wing-drop motions were encountered [1,2]. Lateral instabilities have also occurred in numerous past aircraft development programs, such as for F-84, F-86, A-4, T-45, F-104, T-8, F-4, F-5, F-111, F-15, Harrier, and many others [2–4]. Because these degraded characteristics were not predicted before flight, analysis and solutions of the problems became expensive and difficult [5]. As a result, the joint NASA, U.S. Navy, and U.S. Air Force Abrupt Wing Stall Program was initiated with an objective of identifying flight dynamic deficiencies in the transonic tunnel by employing a free-to-roll (FTR) test rig. The main problem was that the flight dynamic instabilities tended to occur with strong interaction among static and dynamic forces and moments. Therefore, it was not clear whether static testing is adequate to identify all lateral instabilities.

There are three types of uncommanded rolling motions at a transonic speed that have affected many airplanes in the last 60 years. They have been categorized as heavy wing, wing drop, and wing rock. Heavy wing is caused by an asymmetric lift distribution and reduced aileron effectiveness due to shock-induced separation, so that the pilot is forced to increase the aileron deflection and stick force to maintain trim. When the roll trim cannot be maintained, the aircraft begins to roll off [1,2]. Wing drop is irregular and nonperiodic rolling motion. It has been defined as roll-off or “flip” by pilots [6]. Historically, wing-drop problems have mostly been discovered during flight-testing, not in the tunnel. Wing rock is a more periodic type of motion as a limit-cycle oscillation and can be divergent in some cases. It is characterized by highly nonlinear roll damping [1,2,7].

In addition to the preproduction F/A-18E, as indicated earlier, there have been many other configurations and aircraft that have exhibited lateral instabilities in the transonic speed range [8]. For

Presented as Paper 6489 at the Atmospheric Flight Mechanics, Keystone, CO, 21–24 August 2006; received 11 February 2007; revision received 30 January 2008; accepted for publication 5 February 2008. Copyright © 2008 by C. Edward Lan. Published by the American Institute of Aeronautics and Astronautics, Inc., with permission. Copies of this paper may be made for personal or internal use, on condition that the copier pay the \$10.00 per-copy fee to the Copyright Clearance Center, Inc., 222 Rosewood Drive, Danvers, MA 01923; include the code 0021-8669/08 \$10.00 in correspondence with the CCC.

*J. L. Constant Distinguished Professor, Department of Aerospace Engineering, Associate Fellow AIAA.

†Graduate Research Assistant, Department of Aerospace Engineering.

‡Aerospace Engineer, Flight Dynamics Branch, Associate Fellow AIAA.

years, it was thought that airplanes were subjected to uncommanded lateral instabilities only at a high angle of attack. But in reality, the problem is still present even at a low angle of attack (in particular, at transonic speeds [9]). In addition, whenever these nonlinear aerodynamic characteristics dominate, the classical linear flight dynamic theory is inadequate to describe these instabilities. One obstacle in a fighter development program is that these uncommanded lateral motions tended to elude wind-tunnel prediction.

For the purpose of early prediction of lateral instabilities, various figures of merit (FOM) have been reviewed [5,10], including the lift-curve behavior, magnitude of rolling moment and its unsteadiness in rms values, wing-root bending moments, etc. To better correlate the FTR test results to flight data, a new FOM was introduced [10]: $(P_{p-v})_{\max}$, defined as the absolute value of the amplitude change from a peak to its nearest valley divided by the time it takes to roll through this amplitude. However, all these FOM appeared to be unable to correlate reliably with all FTR test results.

Another testing technique proposed by McConnell [11] to identify possible uncommanded lateral instabilities is the continuous-beta-sweep test-and-analysis technique (CBSTAT). It relies on the rolling-moment data acquired by sweeping the model through a range of sideslip angles in both positive and negative directions while holding the angle of attack and Mach number constant. Nonrepeatability, discontinuities, and hysteresis in the rolling-moment data are employed to detect a potential abrupt-wing-stall tendency.

In the present paper, a wing-drop theory is formulated based on the loss of system stiffness in the rolling equation of motion. The FTR data are first corrected for the bearing-friction effects [12], filtered with a method called model-based filtering, and then modeled through a fuzzy-logic algorithm. The resulting roll aerodynamic model is then employed to calculate the damping and stiffness derivatives, including some second-order derivatives, to verify the wing-drop theory.

II. Aerodynamic Modeling

Data from four airplane models (F/A-18E, F-18C, F-16C, and AV-8B) are analyzed in the present investigation. However, for the present paper, only data from the FTR tunnel tests of one airplane model, the preproduction F/A-18E, will be presented. To analyze these data, a suitable method must be capable of capturing possible nonlinear unsteady aerodynamic effects in multiple motion variables. The method used here is based on fuzzy-logic modeling that does not require an assumed functional relationship between aerodynamic coefficients and motion variables and can handle nonlinear interpolation in multiple variables.

In the present investigation, the rolling-moment coefficient is considered to be dependent on the following eight motion variables: α (angle of attack), β (angle of sideslip), ϕ (roll angle), p (roll rate), k [the reduced frequency is $\omega b/(2V)$], M (Mach number), $\dot{\alpha}$ (time rate of the angle of attack), and $\dot{\beta}$ (time rate of the sideslip angle). The fuzzy-logic algorithm uses both the least-squares error and the multiple correlation coefficients to find the most suitable model. The algorithm is summarized in [13,14]. It should be noted that although α , β , and ϕ are related through the kinematic relations, in fuzzy-logic algorithm, they can be considered as linearly independent. The choice of specific independent variables is based on unsteady aerodynamic theory and the study made in [15]. By using the measured roll-angle time history $\phi(t)$ and fitting each segment of 20 points with a harmonic variation, the local oscillation frequency can be estimated. The needed $d\phi/dt$ is estimated with a monotone cubic spline [16]. The vector sum of the measured normal load and the model weight plus counterweight provides the total normal force acting on the bearing. Based on the estimated amplitude of the equivalent harmonic oscillation, frequency, and the normal force, the friction torque can be estimated [12]. The equation of motion is assumed to be of the form

$$I_x \frac{d^2\phi}{dt^2} + \mu \frac{d\phi}{dt} = C_l \bar{q} S b \quad (1)$$

where the right-hand side is measured by the balance. Therefore, the balance measurement must be subtracted by $\mu d\phi/dt$. In addition, the modeled friction torque is always positive. In application, it should have the same sign as $d\phi/dt$.

There are numerous test runs, but only three sets for the preproduction F/A-18E will be analyzed to illustrate different possible lateral instabilities.

A. Data Reduction by Model-Based Filtering of Model F/A-18E

Because of turbulence and model vibration, it is difficult to establish a good model with a high correlation coefficient. When all data points are used, the squared correlation coefficient R^2 is typically between 0.3 and 0.4, except those cases with a wing-rock-like motion. For the latter cases, R^2 can reach a value greater than 0.95. According to statistical analysis, if $R^2 = 0.95$, it implies that 95% of the data is explained by the model [17]. The variance and standard deviation can also be estimated if needed. Therefore, the priority is to find a method to increase the correlation coefficient. A high correlation coefficient will also reduce the scattering of calculated derivatives. In practice, filtering is frequently achieved with a low-pass filter. However, the choice of a cutoff frequency without discarding useful data is not certain. The uncertainty of selecting a correct cutoff frequency is more evident in dynamic testing. Another approach that has been employed in the maximum likelihood method [18] is to not discard any data point. Instead, the error bounds are computed and the estimated stability derivatives are taken to be the mean values.

Based on these considerations, the following method is developed for filtering. In a sense, the present approach is a combination of the two aforementioned methods. That is, the high-frequency data that are not associated with the aerodynamic behaviors will produce a large deviation from the predicted mean curve in the least-squares-error sense and are hence removed. Large deviation from the mean implies a large contribution to the sum of squared errors and hence reduces the correlation coefficient. Instead of taking the mean after the model identification, in the present method, the data are filtered initially to reduce the computing time and to make the estimated stability derivatives smoother with time variation. In the present method, the model structure (i.e., the number of cells representing each variable) is determined, with all data included for each test run. After R^2 remains unchanged in 20,000 iterations or more, all data points that deviate from the model-predicted values by more than a fixed percentage (such as 1000%) will be deleted. The percent deviation is calculated as the ratio of the difference between the model prediction and the data value to the model prediction. In the next run, the percentage of deviation is reduced, and so on, until R^2 reaches a value greater than 0.8. Because the model structure is not changed, the mean characteristics (in the least-sum-of-squared-errors sense) after data filtering will not significantly change when the sample size is large, as is demonstrated in the following example calculations. Because all stability derivatives will be calculated at the remaining data points, the present approach also has the additional advantage of reducing, but not eliminating, the scattering of the estimated derivatives, as indicated earlier. For most cases analyzed here with motions similar to that for test run 319, the final specified filtering percentage is 50%, and the number of remaining data points is between 2000 and 2500 (still quite large). Note that the number of the original data without filtering is usually greater than 6000 in each run. The idea of reducing the number of data points by keeping one record in every two has also been tried. However, the resulting R^2 was still low (less than 0.4).

To illustrate the effect of filtering, consider test run 319. Figure 1 shows the model-predicted results with filtering (solid symbols) compared with the original data (hollow symbols). It is seen that modeling tends to automatically smooth out the data and fit only those significant data points.

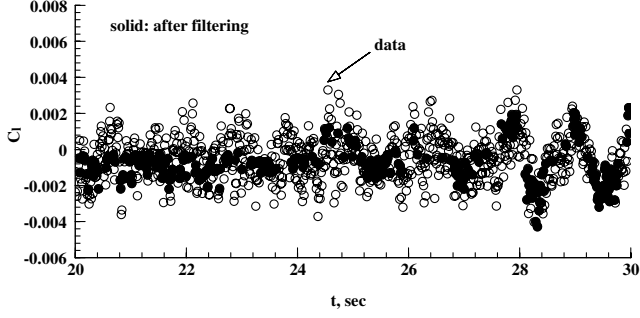


Fig. 1 Comparison of filtered rolling-moment coefficients (solid symbols) with the original data (hollow symbols) for the F/A-18E, run 319; $\delta_{le}/\delta_{te}/\delta_a = 15/10/5$ deg, $M = 0.8$, and $\alpha_i = 7.85$ deg.

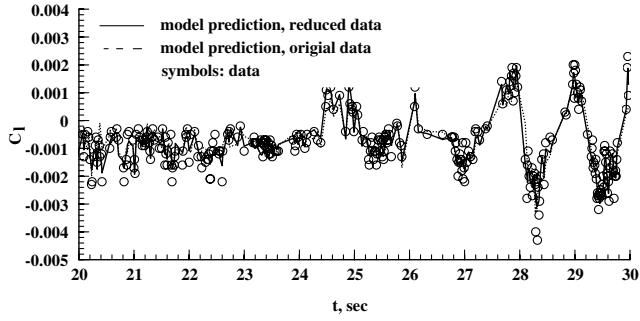


Fig. 2 Comparison of predicted results with a model based on the original data and a model with the filtered data for the F/A-18E, run 319; $\delta_{le}/\delta_{te}/\delta_a = 15/10/5$ deg, $M = 0.8$, and $\alpha_i = 7.85$ deg.

Figure 2 shows that if the original data are not filtered, the resulting model predicts quite similar results, even though R^2 is low (≈ 0.31). The main advantage of filtering is, again, to reduce the computing time and to smooth the calculated derivatives along the time history of motion.

III. Theory of Wing Drop

The following oscillation equation will be assumed in determining the stability of the aircraft model:

$$\frac{I_x \ddot{\phi}}{qSb} - C_{\dot{\phi}} \dot{\phi} + C_{\phi} \phi = C_{l_0} \quad (2)$$

where C_{l_0} is the rolling-moment coefficient at $\phi = \phi_0$, the mean roll angle. The damping and stiffness terms are defined as

$$C_{\dot{\phi}} = \left(C_{l_p} + C_{l_{\dot{\beta}}} \frac{\partial \beta}{\partial \phi} \right) \frac{b}{2V} \quad (3)$$

$$C_{\phi} = C_{l_{\phi}} + C_{l_{\alpha\phi}} \alpha \quad (4)$$

In Eq. (3), the β derivative with ϕ can be obtained with the following kinematic relations:

$$\sin \beta = \sin \phi \sin \theta \quad (5a)$$

$$\tan \alpha = \cos \phi \tan \theta \quad (5b)$$

Differentiating Eq. (5a) gives

$$\frac{\partial \beta}{\partial \phi} = \frac{\cos \phi}{\cos \beta} \sin \theta \approx \tan \alpha \approx \sin \alpha \quad (6)$$

The second derivative with ϕ is not considered in Eq. (4), because to the first order, ϕ^2 will not contribute to the in-phase moment or to

the system stiffness. Note that the derivative $C_{l_{\alpha\phi}}$ was used in a slightly different form in [19] to develop a roll-lock-in theory for missiles, in that when it was able to balance the control rolling moment or the moment due to configurational asymmetry, the vehicle would stop rolling at its banked position. Therefore, in the present notation, roll lock-in would occur if we have

$$C_{l_{\delta a}} \delta_a + C_{l_{\alpha\phi}} \alpha \phi = 0 \quad (7)$$

The reason for using $C_{l_{\alpha\phi}}$ instead of $C_{l_{\phi}}$ in the lock-in theory is that $C_{l_{\delta a}}$ is a function of α . The present theory of wing drop is based on the value of C_{ϕ} [Eq. (4)], and it is applicable to cases with or without asymmetrical aileron deflections. Because there is no control moment to balance in the present experimental data (i.e., all aileron deflections are symmetrical), the value of $C_{l_{\alpha\phi}}$ should be small at the wing-drop conditions. Because roll lock-in conditions do not exist in the present study, the necessary condition for wing drop can be identified as the condition at which the sign of C_{ϕ} is changed. Theoretically, the oscillation equation should be written with respect to an unknown mean roll angle, which is typically not zero. Therefore, the overall sign of C_{ϕ} may be positive or negative. C_{ϕ} will be called the relative stiffness; that is, the magnitude of the stiffness term on the left side of Eq. (2) is relative to C_{l_0} . However, the sign change of C_{ϕ} should not be the result of two large terms with opposite sign. Therefore, the sufficient condition for wing drop is that $C_{l_{\alpha\phi}}$ and $C_{l_{\phi}}$ are of the same sign, and one of them should be small because there is no control moment to balance. In summary, the existence of wing drop in the tunnel testing is determined if the following occur:

1) The sign of C_{ϕ} at some discrete points is changed from the rest of the data points in the motion.

2) The contribution to the rolling-moment coefficient from $C_{l_{\alpha\phi}}$ is of the same sign as that of $C_{l_{\phi}}$ and one of them is small in magnitude.

It should be noted that because all derivatives are calculated at the local flow conditions, dynamic effects such as those due to roll rate are automatically taken into account. Using the terminology of a conventional vibration system, the wing-drop condition corresponds to the condition of a vanishing frequency.

IV. Results and Discussion

Note that for all cases examined, the aileron was set symmetrically, in the same way that the trailing-edge flap and the roll derivatives are calculated at the instantaneous conditions based on a central-difference scheme.

A. F/A-18E, Run 196, $\delta_{le}/\delta_{te}/\delta_a = 8/8/4$ deg, $M = 0.8$, and $\alpha_i = 4.85$ deg

The balance rolling-moment coefficients corrected with friction torque and those due to bearing-friction torque are presented in Fig. 3a with periodic characteristics. The friction corrections are not negligible and vary periodically, because they depend on the oscillation frequency and amplitude. In [10], it was shown that the estimated roll damping without friction corrections was inconsistent with the flight-data-derived values, similar to the finding in [12]. In the latter, it is also shown that the damping derivatives calculated with friction correction are more negative (i.e., stable) than those without correction in a well-damped motion. The amplitude of the wing-rock-like oscillation is not constant as it is in a conventional limit-cycle oscillation (Fig. 3b).

The calculated roll derivatives are presented in Fig. 4. Figure 4a shows that the roll-damping derivative is all negative, but $(C_{l_p})_{osc}$ can be positive and negative (Fig. 4b), in which $(C_{l_p})_{osc}$ is defined as

$$(C_{l_p})_{osc} = C_{l_p} + C_{l_{\dot{\beta}}} \sin \alpha \quad (8)$$

Note that α in Eq. (8) is the local angle of attack. Therefore, a positive $(C_{l_p})_{osc}$ arises from a large positive $C_{l_{\dot{\beta}}}$. Meanwhile, the dihedral effect $C_{l_{\beta}}$ in Fig. 4c, though mostly negative, can also become positive with a varying magnitude. According to the conventional wing-rock theory [20], positive C_{l_p} and negative $C_{l_{\beta}}$ are the necessary conditions for wing rock to occur, and it usually occurs at

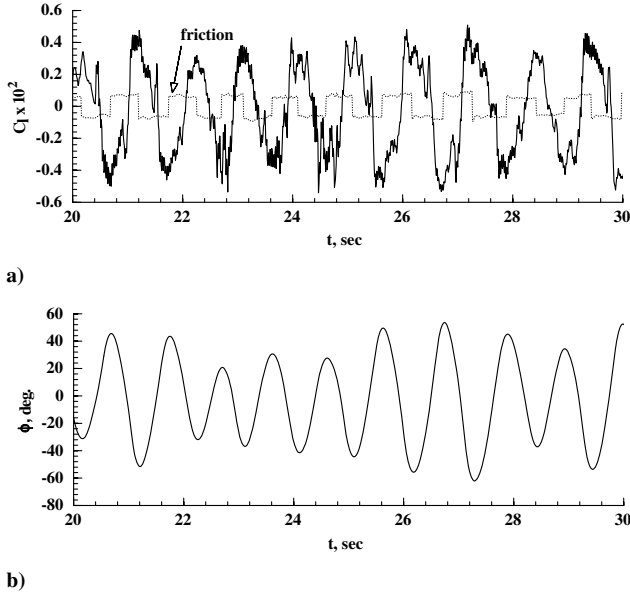


Fig. 3 Values of corrected rolling-moment coefficient and those due to friction, run 196 of the F/A-18E model; $\delta_{le}/\delta_{te}/\delta_a = 8/8/4$ deg, $M = 0.8$, and $\alpha_i = 4.85$ deg.

high α with nonlinear roll damping. In the present case of wing rock in a transonic tunnel at low α , the wing rock appears to be caused by the time rate of change in sideslip, not by the roll rate. Because $C_{l\beta}$ represents the linear stiffness in rolling motion and it varies significantly to result in the variation of frequency, it follows that not

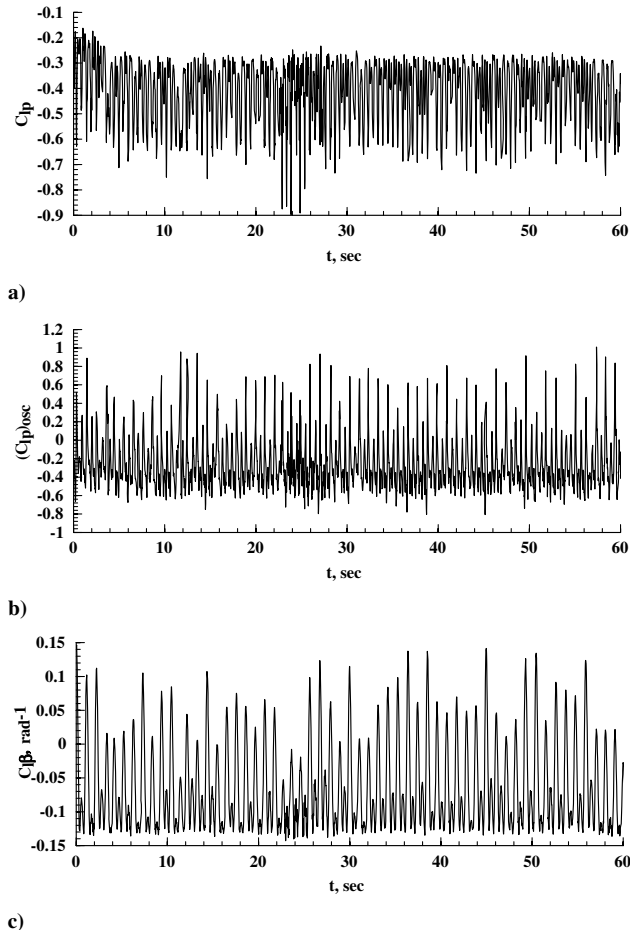


Fig. 4 Calculated roll derivatives for the F/A-18E model in run 196; $\delta_{le}/\delta_{te}/\delta_a = 8/8/4$ deg, $M=0.8$, and $\alpha_i = 4.85$ deg.

only is the roll damping nonlinear due to $C_{l\dot{\beta}}$, but the stiffness [the C_ϕ term, Eq. (4)] is nonlinear as well.

To further explore the possible mechanisms for wing rock in the tunnel, Figs. 5a and 5b present the contributions to C_l from some derivatives that are all defined in the following form:

$$\Delta(C_l) = C_{l\alpha\phi} \times \alpha\phi \quad (9)$$

where α and ϕ are in radians. The contribution from ϕ is calculated as $C_{l\phi} \times \phi$. The derivative $C_{l\phi}$ is similar to $C_{l\beta}$ in its effect on the rolling characteristics, but its effect is more intuitively direct. The contribution to the rolling-moment coefficient from total damping is defined as follows:

$$\Delta(C_l)_{osc} = C_{lp} \left(\frac{pb}{2V} \right) + C_{l\dot{\beta}} \left(\frac{\dot{\beta}b}{2V} \right) \sin \alpha \quad (10)$$

Figures 5a and 5b show that the main contributions are from $C_{l\alpha\phi}$, $C_{l\phi}$, and $C_{l\dot{\beta}}$, and the system relative stiffness C_ϕ is always positive. As indicated in Eq. (4), the magnitudes of both $C_{l\alpha\phi}$ and $C_{l\phi}$ or C_ϕ are the key in causing the wing drop. In the present case, Fig. 5b indicates that the contribution of $C_{l\dot{\beta}}$ to the oscillatory roll-damping derivative [Eq. (8)] has a phase shift to those from $C_{l\alpha\phi}$ and $C_{l\phi}$. When the contributions from $C_{l\alpha\phi}$ and $C_{l\phi}$ are in phase with the roll angle, the derivatives should be all positive, implying a positive relative stiffness C_ϕ . Therefore, the motion is wing rock, not wing drop. It may be concluded that in a wing rock, the nonlinear relative stiffness C_ϕ is positive, but behaves in an oscillatory manner so that the system frequency is not constant. At the same time, the nonlinear damping is also significant and varying periodically.

B. F/A-18E, Run 319, $\delta_{le}/\delta_{te}/\delta_a = 15/10/5$ deg, $M = 0.8$, and $\alpha_i = 7.85$ deg

In this case, the initial angle of attack is higher than in the previous case by 3 deg. The corrected balance rolling moment and the friction

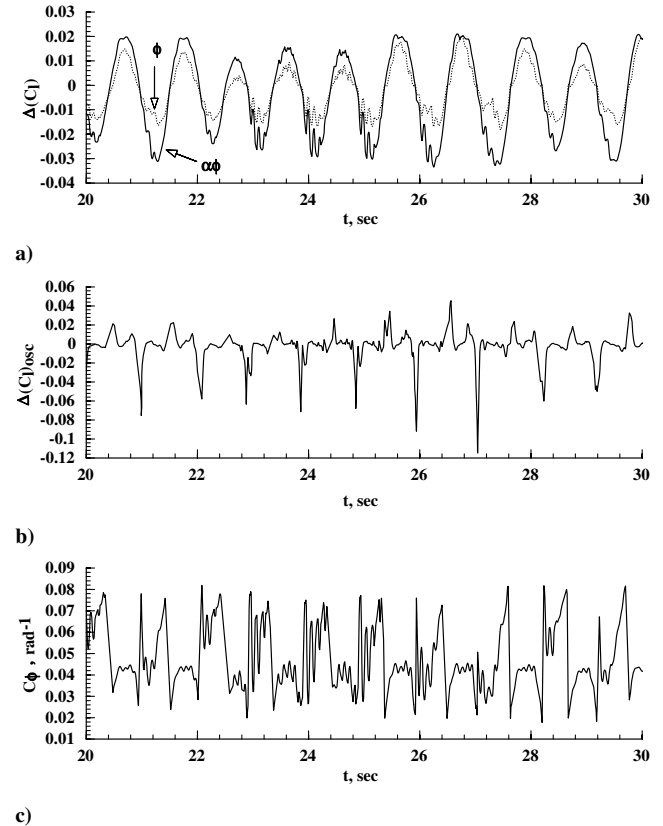


Fig. 5 Contributions of various roll derivatives to the total rolling-moment coefficient for the F/A-18E model, run 196; $\delta_{le}/\delta_{te}/\delta_a = 8/8/4$ deg, $M = 0.8$, and $\alpha_i = 4.85$ deg.

corrections are shown in Fig. 6a and appear to be chaotic. The friction corrections are small (Fig. 6a). The motion is not wing rock (Fig. 6b). Figure 7 illustrates the variation of roll derivatives. It is seen that the roll-damping derivatives due to roll rate are again all negative [i.e., stable (Fig. 7a)], but $C_{l\dot{\beta}}$ can occasionally become large and positive based on the large positive values of $(C_{lp})_{osc}$ (Fig. 7b). In addition, the dihedral effect is always stable [i.e., negative (Fig. 7c)]. Therefore, based on the traditional definition of roll derivatives (in particular, $C_{l\beta}$), it will not be possible to determine the occurrence of wing drop. On the other hand, as shown in Fig. 8, when the relative stiffness C_ϕ becomes negative, wing drop is possible, because it occurs at t slightly greater than 50 s and other time instants. One important feature of C_ϕ characteristics is that they do not vary as

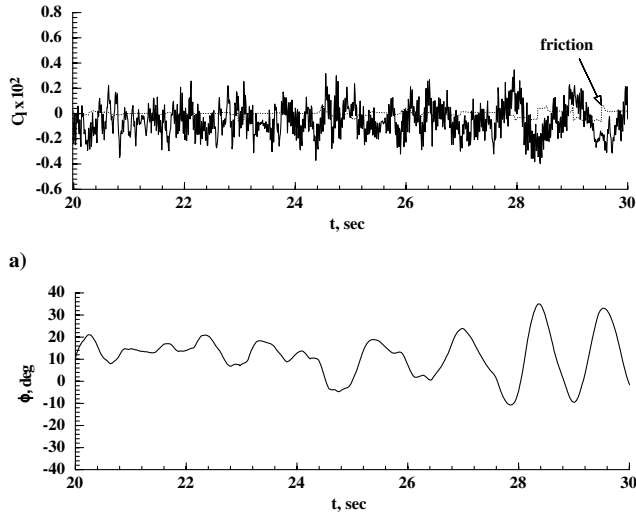


Fig. 6 Values of friction-corrected rolling-moment coefficient and that due to friction in run 319 of the F/A-18E model; $\delta_{le}/\delta_{te}/\delta_a = 15/10/5$ deg, $M = 0.8$, and $\alpha_i = 7.85$ deg.

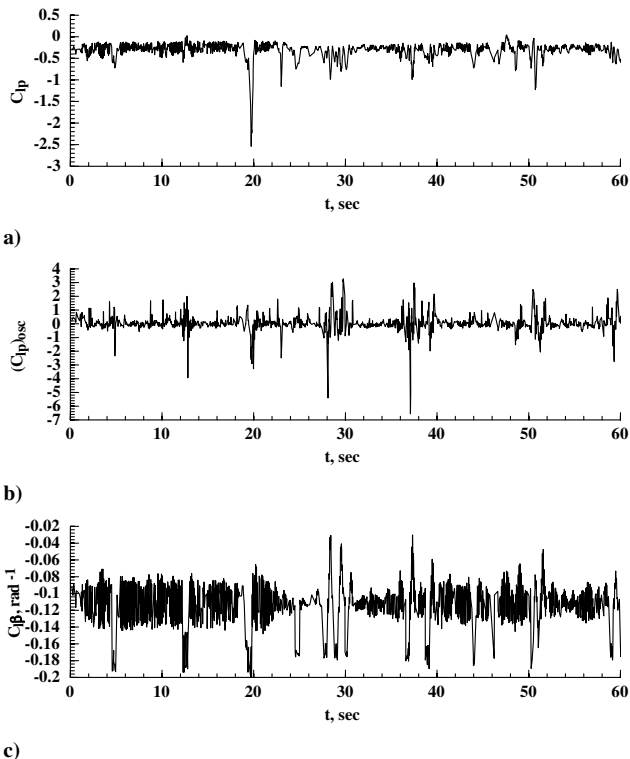


Fig. 7 Variation of roll derivatives in run 319 of the F/A-18E model; $\delta_{le}/\delta_{te}/\delta_a = 15/10/5$ deg, $M = 0.8$, and $\alpha_i = 7.85$ deg.

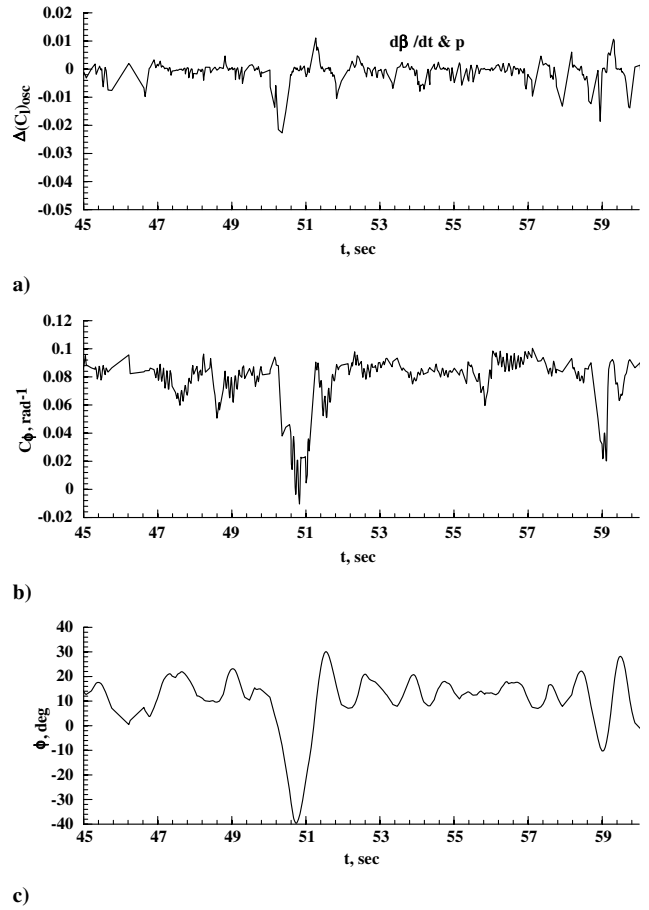


Fig. 8 Contributions of various roll derivatives to the total rolling-moment coefficient in run 319 of the F/A-18E model (interval of time is 45–60 s); $\delta_{le}/\delta_{te}/\delta_a = 15/10/5$ deg, $M = 0.8$, and $\alpha_i = 7.85$ deg.

much as those in run 196 (Fig. 5): only occasional spikes exist. A detailed examination of the computed data indicates that within the following periods around the indicated time, C_ϕ is negative. Noting that $\Delta(C_l)_{\alpha\phi}$ is defined in Eq. (9) and, together with $\Delta(C_l)_\phi$, these two parameters indicate the relative contributions to the rolling-moment coefficient during the motion at $t = 12.76$ s:

$$[\Delta(C_l)_{\alpha\phi}, \Delta(C_l)_\phi] = [0.00204, -0.00168]$$

and

$$[C_{l\alpha\phi}, C_{l\phi}] = [-0.08259, 0.00924]$$

On the other hand, at $t = 50.717$ s,

$$[\Delta(C_l)_{\alpha\phi}, \Delta(C_l)_\phi] = [0.00088, 0.00068]$$

and

$$[C_{l\alpha\phi}, C_{l\phi}] = [-0.01171, -0.00099]$$

According to the present wing-drop theory, wing drop occurs when the contribution to the rolling-moment coefficient from $C_{l\alpha\phi}$ is of the same sign as that of $C_{l\phi}$ and one of them is small in magnitude. This condition is satisfied at $t = 50.717$ s, as shown in Fig. 9 and in Fig. 8b with a negative value of C_ϕ [Eq. (4)]. However, in the time period around $t = 12.76$, $\Delta(C_l)_{\alpha\phi}$ and $\Delta(C_l)_\phi$ are of opposite sign; therefore, there is no wing drop predicted at $t = 12.76$. Because $(C_{lp})_{osc}$ is large and positive (Fig. 7b) ahead of this time instant ($t = 50.717$), implying a large and positive $C_{l\dot{\beta}}$, this result agrees with that of CBSTAT test results described in [11], in that $C_{l\dot{\beta}}$ is a necessary, but not a sufficient, condition to predict wing drop, because at $t = 12.76$ and many other time instants (Fig. 7b), $C_{l\dot{\beta}}$ is

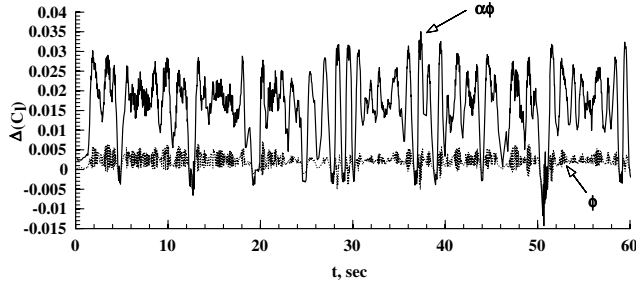


Fig. 9 Variation of contributions to rolling-moment coefficient from static roll derivatives in run 319 of the F/A-18E model; $\delta_{le}/\delta_{te}/\delta_a = 15/10/5$ deg, $M = 0.8$, and $\alpha_i = 7.85$ deg.

also positive without wing drop being predicted. In some of the latter cases, the resulting motions may be nondivergent nonlinear oscillations at the local (α, β) conditions. Positive $C_{l\beta}$ is also exhibited in wing rock (Fig. 4).

C. F/A-18E, Run 376, $\delta_{le}/\delta_{te}/\delta_a = 15/10/5$ deg, $M = 0.8$, and $\alpha_i = 9.57$ deg

In this case, the initial angle of attack is higher than that of the second case by 1.72 deg. Figure 10 presents the calculated roll-stability derivatives as a function of time for this run. Figure 10a shows that the roll-damping derivative due to roll rate is all negative and thus stable. On the other hand, the oscillatory derivatives $(C_{lp})_{osc}$ exhibit large fluctuation from positive to negative values (Fig. 10b). A large positive value of $(C_{lp})_{osc}$ is seen to be associated with a positive value of $C_{l\beta}$ (Fig. 10c).

To examine possible existence of wing drop, the contributions to C_l from damping derivatives and the roll stiffness derivatives are presented in Fig. 11. Figure 11a shows that the contribution from roll damping is oscillatory and significant when compared with that in Fig. 4 in wing-rock motion. Figure 11b indicates that C_ϕ is mostly negative, perhaps because of the large mean roll angle (see Fig. 11c). In the present hypothesis of wing-drop identification, it occurs when

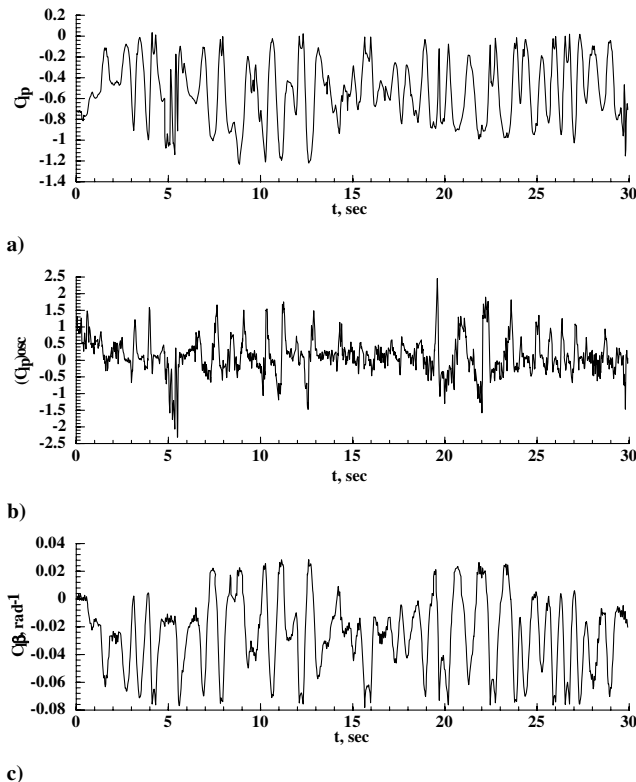


Fig. 10 Calculated roll derivatives for the F/A-18E model in run 376; $\delta_{le}/\delta_{te}/\delta_a = 15/10/5$ deg, $M = 0.8$, and $\alpha_i = 9.57$ deg.

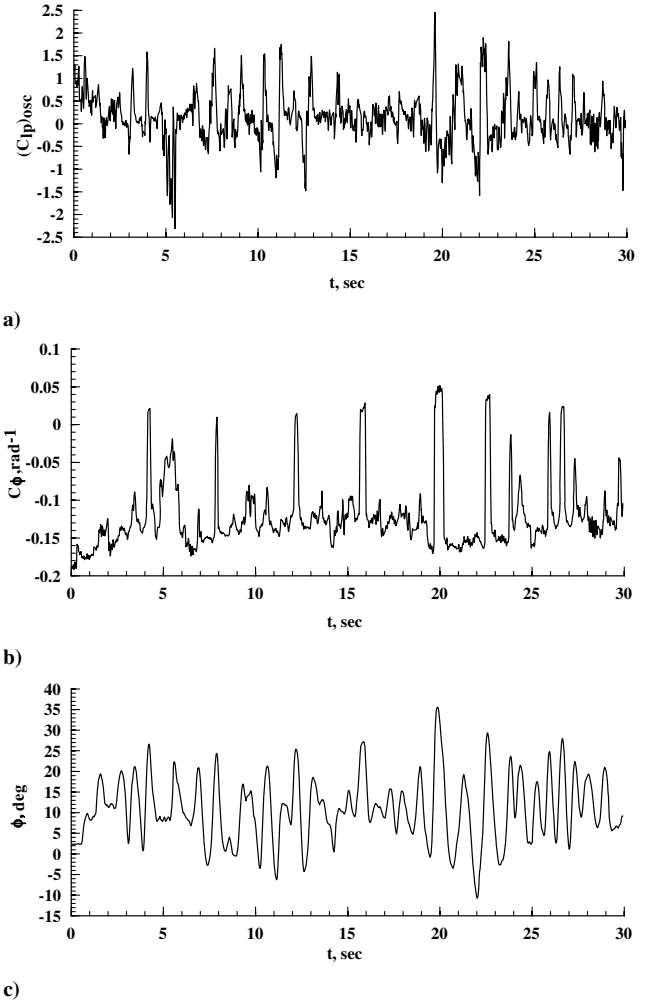


Fig. 11 Contributions of various roll derivatives to the total rolling-moment coefficient for the F/A-18E model (run 376); $\delta_{le}/\delta_{te}/\delta_a = 15/10/5$ deg, $M = 0.8$, and $\alpha_i = 9.57$ deg.

C_ϕ is negative or the sign of C_ϕ changes, the contributions to C_l from $C_{l\alpha\phi}$ and $C_{l\phi}$ are of the same sign, and the magnitude of the $C_{l\alpha\phi}$ contribution is small. Figure 11b indicates that the condition of sign changes in C_ϕ occurs at several time instants t with the corresponding $\Delta(C_l)_{\alpha\phi}$ values: $\Delta(C_l)_{\alpha\phi} = 4.16, 0.00003; 12.24, 0.00001; 15.79, 0.00026; 19.74, 0.00326; 22.48, 0.00107; 25.941, 0.00003; \text{ and } 26.571, 0.00007$.

The corresponding $\Delta(C_l)_\phi$ values stay nearly constant, ranging from 0.0069 to 0.00616, except at times $t = 19.74$ when it is 0.00871 and at $t = 22.48$ when it is 0.00667. In other words, at all these time instants, the contributions to C_l from $C_{l\alpha\phi}$ and $C_{l\phi}$ are of the same sign. These points coincide with those having sign changes in C_ϕ (Fig. 11b). Therefore, wing drop is predicted to occur at the specified flow conditions for this configuration. The magnitude of roll-off angles tend to change with time in an erratic manner (Fig. 11c). Figure 11a also shows that preceding the wing drops, there are times with large positive $(C_{lp})_{osc}$ values. It also indicates that to identify wing-drop conditions based on the FTR data, static characteristics alone (such as C_{lb}) are inadequate.

V. Conclusions

A wing-drop theory was formulated to examine the transonic tunnel data with a free-to-roll test rig to identify possible uncommanded rolling motions. The theory was based on the loss of nonlinear aerodynamic stiffness in the rolling equation of motion. The balance readings were first improved by accounting for the friction torque at the bearing of the test rig. Some of the data points

contaminated by model vibration were removed by a model-based filtering technique that was developed based on the concept of data correlation. The resulting aerodynamic roll models were analyzed through the instantaneous roll derivatives to determine various conditions at which uncommanded rolling motion could occur. Three test runs for the preproduction F/A-18E model were examined in this paper in detail. The results indicated that the preproduction F/A-18E at a low angle of attack with low leading and trailing flap angles at transonic Mach numbers could develop wing rock. It was shown that wing rock was induced by nonlinear roll damping, mainly due to the time rate of sideslip angle, not the roll rate. The nonlinear aerodynamic stiffness was modeled by the sum of the derivatives of rolling-moment coefficient with the roll angle (linear first-order derivative) and the second derivatives of the rolling-moment coefficient with the angle of attack and roll angle. The results indicated that as the angle of attack was increased from a low value at which wing rock was exhibited at a transonic Mach number, wing drop started to occur, initially with a single event and then with multiple occurrences of wing drop at a higher angle of attack, with the magnitude of roll-off angles changing with time. Because nonlinear roll damping played a role in developing wing drop, the occurrence of the latter corresponded to the vanishing of a frequency with damping in the conventional vibration theory and resulted in the need for dynamic data to predict wing-drop behavior.

Acknowledgments

This research was supported by grant NNL04AA23G from NASA Langley Research Center for the first two authors. The computing time was provided by the Center for Advanced Scientific Computing at the University of Kansas.

References

- [1] Hall, R. M., and Woodson, S. H., "Introduction to the Abrupt Wing Stall (AWS) Program," *Journal of Aircraft*, Vol. 41, No. 3, May–June 2004, pp. 425–435.
doi:10.2514/1.3630
- [2] Chambers, J. R., and Hall, R. M., "Historical Review of Uncommanded Lateral-Directional Motions at Transonic Conditions," *Journal of Aircraft*, Vol. 41, No. 6, Nov.–Dec. 2004, pp. 1266–1274.
doi:10.2514/1.9839
- [3] McMillin, S. N., Hall, R. M., and Lamar, J. E., "Transonic Experimental Observations of Abrupt Wing Stall on F/A-18 Model," *Journal of Aircraft*, Vol. 42, No. 3, May–June 2005, pp. 586–599.
doi:10.2514/1.3152
- [4] Schuster, D. M., and Byrd, J. E., "Transonic Unsteady Aerodynamics of the F/A-18E at Conditions Promoting Abrupt Wing Stall," *Journal of Aircraft*, Vol. 41, No. 3, May–June 2004, pp. 485–492.
doi:10.2514/1.4305
- [5] Lamar, J. E., Capone, F. J., and Hall, R. M., "AWS Figure of Merit (FOM) Developed Parameters from Static, Transonic Model Tests," AIAA Paper 2003-0745, Jan. 2003.
- [6] Jones, J. G., "Aircraft Aerodynamics Response Associated with Fluctuating Flow Fields," AGARD Lecture Series No. 74, 1975.
- [7] Ericsson, L. E., "Various Sources of Wing Rock," *Journal of Aircraft*, Vol. 27, No. 6, Nov.–Dec. 1990, pp. 488–494.
- [8] Borchers, P. F., Franklin, J. A., and Fletcher, J. W., "Flight Research at Ames: Fifty-Seven Years of Development and Validation of Aeronautical Technology," NASA SP-3300, 1998.
- [9] Sreenatha, A. G., Nair, N. K., and Sudhakar, K., "Aerodynamic Suppression of Wing Rock Using Fuzzy Logic Control," *Journal of Aircraft*, Vol. 37, No. 2, Mar.–Apr. 1999, pp. 345–348.
- [10] Capone, F. J., Hall, R. M., Owens, D. B., Lamar, J. E., and Mcmillin, S. N., "Review and Recommended Experimental Procedures for Evaluation of Abrupt Wing Stall Characteristics," *Journal of Aircraft*, Vol. 41, No. 3, May–June 2004, pp. 456–463.
doi:10.2514/1.1449
- [11] McConnell, J. K., "Continuous Beta Sweep Test and Analysis Technique (CBSTAT) for Predicting Wing Drop Based on Static Wind Tunnel Testing," AIAA Paper 2004-5048, Aug. 2004.
- [12] Lan, C. E., Bianchi, S., and Brandon, J. M., "Effects of Bearing Friction of a Free-to-Roll Test Rig on Transonic Lateral Aerodynamics," *Journal of Aircraft*, Vol. 45, No. 1, Jan.–Feb. 2008, pp. 298–305.
- [13] Wang, Z., Lan, C. E., and Brandon, J. M., "Fuzzy Logic Modeling of Nonlinear Unsteady Aerodynamics," AIAA Paper 1998-4351, Aug. 1998.
- [14] Lan, C. E., Li, J., Yau, W., and Brandon, J. M., "Longitudinal and Lateral-Directional Coupling Effects on Nonlinear Unsteady Aerodynamic Modeling from Flight Data," AIAA Paper 2002-4804, Aug. 2002.
- [15] Lan, C. E., and Brandon, J. M., "Development of Nonlinear Aerodynamic Models from Flight Data and Evaluation of Tabulated Aerodynamic Models," AIAA Paper 2003-5696, Aug. 2000.
- [16] Huynh, H. T., "Accurate Monotone Cubic Interpolation," *SIAM Journal on Numerical Analysis*, Vol. 30, No. 1, Feb. 1993, pp. 57–100.
doi:10.1137/0730004
- [17] Barnes, J. W., *Statistical Analysis for Engineers and Scientists*, McGraw-Hill, New York, 1994, p. 218.
- [18] Iliff, K. W., and Wang, K-S, C., "Extraction of Lateral-Directional Stability and Control Derivatives for the Basic F-18 Aircraft at High Angles of Attack," NASA TM 4786, Feb. 1997.
- [19] Nicolaides, J. D., "A Review of Some Recent Progress in Understanding Catastrophic Yaw," AGARD Report 551, Neuilly-sur-Seine, France, 1966.
- [20] Hsu, C. H., and Lan, C. E., "Theory of Wing Rock," *Journal of Aircraft*, Vol. 22, Oct. 1985, pp. 920–924.